Structural Engineering and Mechanics, *Vol. 52, No. 3 (2014) 633-646*
DOI: http://dx.doi.org/10.12989/sem.2014.52.3.633

Semi-analytical numerical approach for the structural dynamic response analysis of spar floating substructure for offshore wind turbine

Jin-Rae Cho*, Bo-Sung Kim, Eun-Ho Choi, Shi-Bok Lee and O-Kaung Lim

School of Mechanical Engineering, Pusan National University, Busan 609-735, Korea

(Received April 22, 2014, Revised July 6, 2014, Accepted October 9, 2014)

Abstract. A semi-analytical numerical approach for the effective structural dynamic response analysis of spar floating substructure for offshore wind turbine subject to wave-induced excitation is introduced in this paper. The wave-induced rigid body motions at the center of mass are analytically solved using the dynamic equations of rigid ship motion. After that, the flexible structural dynamic responses of spar floating substructure for offshore wind turbine are numerically analyzed by letting the analytically derived rigid body motions be the external dynamic loading. Restricted to one-dimensional sinusoidal wave excitation at sea state 3, pitch and heave motions are considered. Through the numerical experiments, the time responses of heave and pitch motions are solved and the wave-induced dynamic displacement and effective stress of flexible floating substructure are investigated. The hydrodynamic interaction between wave and structure is modeled by means of added mass and wave damping, and its modeling accuracy is verified from the comparison of natural frequencies obtained by experiment with a 1/100 scale model.

Keywords: spar floating substructure; wave-induced excitation; pitch and heave motions; flexible structural dynamic responses; semi-analytical numerical approach

1. Introduction

Wind turbines for extracting the renewable energy from wind were initially designed to be installed on land, and those showed the rapid increase in both the total number of installation and the maximum wind power capacity to some extent (Hansen and Hansen 2007). However, this rapid increase has been declined owing to several obstacles such as the substantial environmental impact on people living around the wind turbines and the limitation of being high-capacity. Such a restrictive situation naturally turned the attention to the offshore sites, a less restrictive place capable of providing more stable wind of high quality. In general, offshore wind turbines are classified into two categories, fixed- and floating-type depending on how the wind turbine is supported, and the floating-type is again divided into three kinds; barge, tension leg (TLP) and spar according to the type of floating substructure (Lee 2008, Jonkman 2009). The current study is concerned with the spar-type floating offshore wind turbine.

Differing from the fixed-type, the floating-type is still under the on-site proving experiment

*Corresponding author, Professor, E-mail: jrcho@pusan.ac.kr

http://www.techno-press.org/?journal=sem&subpage=8 ISSN: 1225-4568 (Print), 1598-6217 (Online)

stage because several core technologies are not fully settled down (Karimirad *et al*. 2011), particularly the securing of dynamic stability and structural strength to wave and wind loads. The dynamic stability of floating offshore wind turbine is meant by the station keeping at sea and the rotational oscillation (Tong 1998). The station keeping has been traditionally secured by mooring lines, while the rotational oscillation has been suppressed by adjusting the center positions of gravity and buoyancy and the fairlead position for mooring lines (Jeon 2013). The dynamic stability has been traditionally evaluated in terms of time or/and frequency response (i.e., the response amplitude operator (RAO)) of the rigid-body motions of platform. This subject has been intensively studied by experimentally using scale models (Utsunomiya 2010, Goopee *et al*. 2012), by analytically/numerically with the simplified wind turbine geometry and the analytically derived wind/wave loads (Tracy 2001, Jensen *et al*. 2011), or by the combined use of CFD, hydro, FSI (fluid-structure interaction) or/and MBD (multibody dynamics) codes (Jonkman and Musial 2010, Wang and Sweetman 2012).

Contrary to the dynamic stability, the study on structural strength to wave and wind loads has been rarely reported. The structural failure of floating substructure of offshore wind turbine not only results in the loss of wind power generation performance but also leads to the tremendous financial expense for repairing or recovering at sea. One of reasons why this subject is behind the concern of investigators is owing to the reorganization that it is relatively less important than the dynamic stability and the complexity of structural dynamic analysis of floating structure. Here, the complexity is caused by the interaction between fluid flow and structural dynamic deformation, which inevitably requires the employment of time-consuming painstaking fluid-structure interaction simulation. In this context, a simple but reliable structural dynamic analysis method is desired to evaluate the structural strength as well as the dynamic stability of floating platform subject to wave or/and wind excitations.

The purpose of this paper is to introduce a semi-analytical numerical approach for analyzing the structural dynamic response of spar floating substructure for offshore wind turbine subject to wave-induced excitation. The time responses of rigid floating platform at the center of mass are analytically solved using the dynamic equations of rigid ship motion (Biran 2003). Meanwhile, the dynamic displacement and stresses are numerically obtained by finite element analysis for which the analytically-solved rigid body motions are input as external dynamic excitations. The approach is motivated by the fact that the displacement of flexible body is composed of the deformation and the rigid body motion, where only the deformation produces strains and stresses. For the illustration purpose of this approach, pitch and heave motions are considered in the current study, by restricting the wave excitation to one-dimensional sinusoidal harmonic motion at sea state 3. Not only the wave-induced pitch and heave motions of floating substructure but also the wave-induced dynamic displacements and effective stress are analyzed and investigated by the proposed method.

2. Problem description

2.1 Structural dynamic response of spar floating wind turbine

Fig. 1(a) shows a typical spar-type floating offshore wind turbine supported by the buoyancy force produced by the hollow cylindrical floating substructure. The wind tower supporting the upper part and the floating substructure is assembled such that the assembling interface is

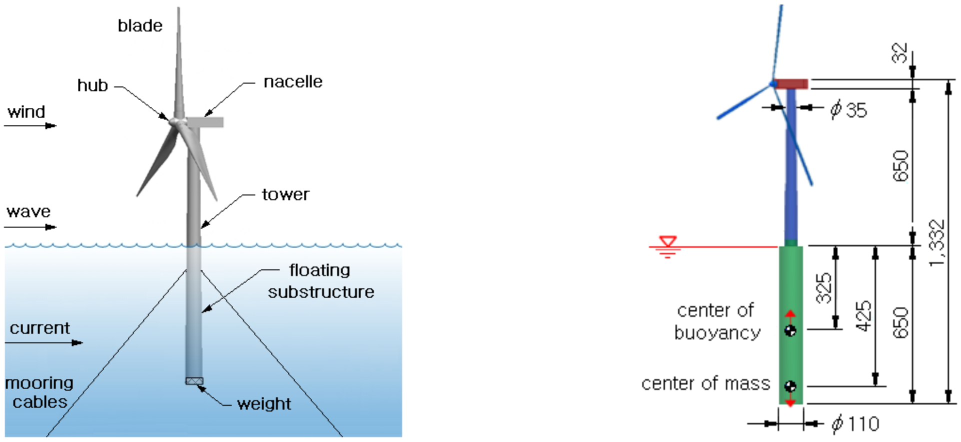

(a) (b)

Fig. 1 Spar-type floating offshore wind turbine: (a) major components, (b) 1/100 scale model (unit: mm)

positioned just below the water free surface. Differing from the fixed-type, the floating-type may exhibit the remarkably unstable dynamic response in the horizontal, vertical and rotational directions when it is subject to unstable wind, wave and current loads (Faltinsen 1990). The dynamics stability of the floating wind turbine is usually meant by the station keeping at sea and the stable rotational attitude (Tong 1998). The station keeping is maintained by thee mooring cables connected to the substructure, while the rotational oscillation is suppressed by adjusting the center positions of mass and buoyancy and the connection position of mooring cables. The ballast weight at the bottom is used to lower the center of mass because the rational stiffness increases in proportional to the relative distance between the center of mass and the center of buoyancy (Koo *et al*. 2004, Karimirad *et al*. 2011). Regarding the connection position of mooring cables, it has been reported from the numerical simulation that the position at or just above the center of buoyancy could minimize the rotational oscillation (Jeon *et al*. 2013). In addition, further suppression of rotational oscillation could be made by installing the passive or active damper to the wind tower or the floating substructure (Lee *et al*. 2006, Colwell and Basu 2009).

The above mentioned dynamic stability is evaluated in terms of time or/and frequency response (i.e., the response amplitude operator (RAO)) of the rigid-body motions of platform. But, what is no less important is to secure the structural strength to the dynamic impact loads of wave and wind, nevertheless the study on this subject has been rarely reported. One of reasons why such a subject is behind the concern of investigators is owing to the complexity of structural dynamic analysis of floating structure. Here, the complexity is meant by the interaction between fluid flow and structural motion, which inevitably requires the use of time-consuming painstaking fluid-structure interaction simulation. In this context, a simple but reliable structural dynamic analysis method is desired to evaluate the structural strength as well as the dynamic stability of floating platform. The reliability of the numerical simulation is made by the comparison with the experiment, even though restricted to the natural frequencies, but unfortunately the experiment using a full-scale or even a proto-type floating platform is not available at the current stage. Thus, the only way is to utilize the experiment in an in-door wave tank using a scale model (Utsunomiya 2010, Goopee *et al*. 2012), and Fig. 1(b) shows the major dimensions of a 1/100 scale model under consideration for the current study.

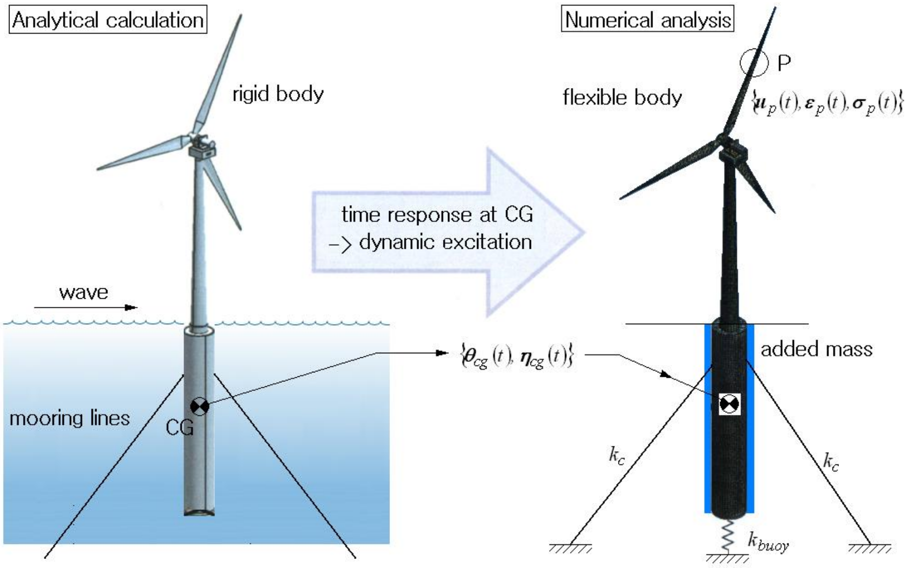

Fig. 2 Schematic representation of the semi-analytical numerical approach

2.2 Motivation and concept

The concept of the semi-analytical numerical approach is schematically represented in Fig. 2, where a floating wind turbine is assumed to be rigid for the analytical calculation while its flexibility is fully considered in the finite element structural dynamic analysis. This approach is motivated by the following two facts. First, the displacement of flexible body is composed of the deformation and the rigid body motion, where only the deformation produces strains and stresses. Second, the rigid body motion of floating platform can be analytically solved from the equations of rigid ship motion (Biran 2003, Cho *et al*. 2012), and it can be replaced with the external excitation for the problem solving the structural deformation. In the analytical calculation, the time responses of rigid body motions $\{\boldsymbol{\theta}_{cg}(t), \boldsymbol{\eta}_{cg}(t)\}$ of floating platform at the center of gravity are obtained by solving the matrix equations of rigid ship motion. Here, $\boldsymbol{\theta}_{cg}(t)$ indicates the time responses of three rigid-body translation motions, while $\boldsymbol{\eta}_{cg}(t)$ denotes those of three rigid-body rotational motions.

Next, in order for the numerical analysis, the analytically-calculated time responses of rigid body motions are applied to the center of gravity as external excitations. The flexible wind turbine system is assumed to be linearly elastic, and the hydrodynamic interaction between wave and structure is simplified as added mass while both mooring lines and buoyancy force are modeled as linear springs with the spring constants k_c and k_{buoy} respectively. The wind load could be also applied to the wind tower, rotor blades and nacelle by making use of Morrison's equation for relative motion (Li and Kareem 1990). The determination of spring constant k_c of linear mooring cables is straightforward (i.e., $k_c=EA$, where E and A are Young's modulus and the cross-section area, respectively), while the spring constant k_{buoy} is calculated by dividing the total buoyancy force with the cross-section area of platform. Once a FE structural dynamic model is establish, the time responses of displacement, strains and stresses $\boldsymbol{u}_p(t)$, $\boldsymbol{\varepsilon}_p(t)$ and $\boldsymbol{\sigma}_p(t)$ at any point P in the floating wind turbine could be easily obtained using a non-specific general FEM code.

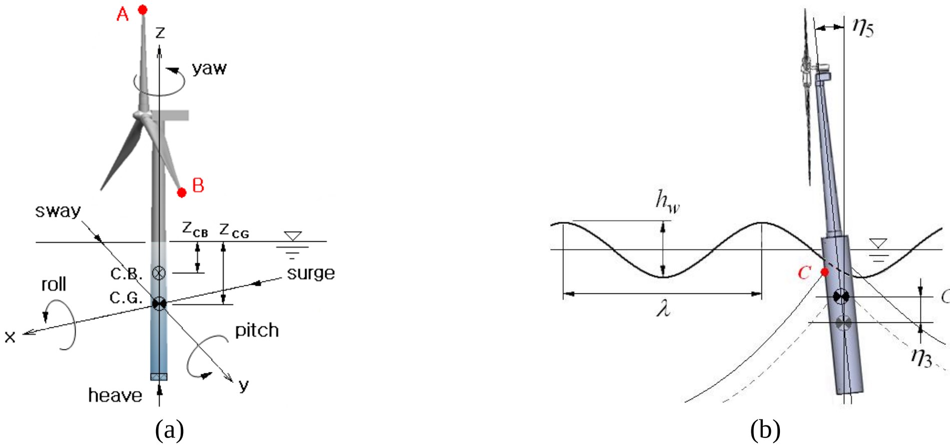

Fig. 3 (a) Rigid body motion with 6 DOFs, (b) rigid pitch and heave motions of spar floating wind turbine by one-dimensional sinusoidal beam wave.

3. Two-step analytical numerical analysis method

3.1 Analytical derivation of wave-induced pitch and heave motions

Referring to Fig. 3(a), the rigid ship motion $\boldsymbol{R} \in \Re^3$ of floating offshore wind turbine is decomposed into the rigid translation $\boldsymbol{s} \in \Re^3$ and the rigid rotation $\boldsymbol{\Omega} \in \Re^3$ such that

$$\boldsymbol{R} = \boldsymbol{s} \oplus \boldsymbol{r} \times \boldsymbol{\Omega} \tag{1}$$

$$\boldsymbol{s} = \eta_1 \boldsymbol{i} + \eta_2 \boldsymbol{j} + \eta_3 \boldsymbol{k}\ , \quad \boldsymbol{\Omega} = \eta_4 \boldsymbol{i} + \eta_5 \boldsymbol{j} + \eta_6 \boldsymbol{k} \tag{2}$$

In which η_1, η_2 and η_3 denote surge, sway and heave motions, while η_4, η_5 and η_6 indicate roll, pitch and yaw motions, respectively.

Introducing the (6×6) wave and viscous damping matrices $\boldsymbol{B}$ and $\boldsymbol{b}$, the added mass (or, moment of inertia) matrix $\boldsymbol{m}^a$ and the restoring stiffness matrix $\boldsymbol{C}$, the generalized coupled rigid ship motions are expressed by (Biran 2003)

$$\left(\boldsymbol{M} + \boldsymbol{m}^{a}\right)\ddot{\eta} + \left(\boldsymbol{B} + \boldsymbol{b}\delta_{4j}\right)\dot{\eta} + \boldsymbol{C}\eta = Re\left(\boldsymbol{F}e^{i\omega_E t}\right) \tag{3}$$

In which, $\boldsymbol{M}$ and $Re\left(\boldsymbol{F}^{-i\omega_E t}\right)$ denote the structure mass (or, moment of inertia) matrix and the vector of sinusoidal exciting force and moment. In addition, the encounter frequency ω_E is calculated by $\omega_E = \omega_w - \omega_w^2 u \cos\mu / g$ with the wave frequency ω_w, the structure moving velocity u and the encounter angle μ. The water viscous damping is known to be remarkable in rotational motion, when compared to the wave damping, but its effect on the rotational motion disappears when the flow is assumed to be inviscid.

According to the Pierson-Moskowitz sea spectrum (1964), the wave length λ, the wave height h_w and the wave frequency ω_w at sea state 3 are known as λ=14.02~16.0 m, h_w=1.07~1.22 m and ω_w=1.57~1.80 rad/sec. These sea conditions are taken because floating offshore wind turbine should be under normal operating at this sea state. The fact that the wind power efficiency reaches its peak when the rotor axis is aligned to the wind direction informs that the floating offshore wind turbine is sensitive to the pitch motion. Meanwhile, the wave length is not small compared to the diameter of floating substructure so that the heave motion can not be ignored. So, for the current study, we consider only the rigid pitch and heave motions of floating offshore wind turbine subject to a uni-directional harmonic wave excitation in the negative *x*-direction, as shown in Fig. 3(b).

Neglecting the coupling with the roll motion and using the relation of $\omega_E=\omega_w$, the coupled rigid heave and pitch motions are expressed by (Lee 2003)

$$\begin{bmatrix} M + m_{33}^a & m_{35}^a \\ m_{53}^a & I_{55} + J_{55}^a \end{bmatrix} \begin{Bmatrix} \ddot{\eta}_3 \\ \ddot{\eta}_5 \end{Bmatrix} + \begin{bmatrix} B_{33} & B_{35} \\ B_{53} & B_{55} \end{bmatrix} \begin{Bmatrix} \dot{\eta}_3 \\ \dot{\eta}_5 \end{Bmatrix} + \begin{bmatrix} C_{33} & C_{35} \\ C_{53} & C_{55} \end{bmatrix} \begin{Bmatrix} \eta_3 \\ \eta_5 \end{Bmatrix} = \begin{Bmatrix} Re\left(F_3 e^{i\omega_w t}\right) \\ Re\left(F_5 e^{i\omega_w t}\right) \end{Bmatrix} \tag{4}$$

with M and m_{33}^a being the total mass and the total added mass of the floating wind turbine and I_{55} and J_{55}^a being the pitch moment of inertia and the added pitch moment of inertia, respectively. Here, m_{ij}^a, B_{ij} and C_{ij} (ij=35, 53) denote the added masses, wave damping coefficients and restoring stiffness coefficients caused by the coupling between heave and pitch motions. These terms could be neglected when the wave height is small and the structure slenderness is large, then Eq. (4) ends up with two uncoupled equations given by

$$\left(M + m_{33}^a\right)\ddot{\eta}_3 + B_{33}\dot{\eta}_3 + C_{33}\eta_3 = Re\left(F_3 e^{i\omega_w t}\right) \tag{5}$$

$$\left(I_{55} + J_{55}^a\right)\ddot{\eta}_5 + B_{55}\dot{\eta}_5 + C_{55}\eta_5 = Re\left(F_5 e^{i\omega_w t}\right) \tag{6}$$

Letting ρ and W be the density and the total weight of the floating wind turbine, the heave and pitch restoring stiffness coefficients C_{33} and C_{55} are calculated by $C_{33}=\rho g A_w$ and $C_{55} = W \cdot \overline{GZ}_L$, respectively. Here, A_w and $\overline{GZ}_L$ indicate the cross-section area and the lateral righting arm of the floating substructure. Then, the natural angular frequencies of heave and pitch motions are defined by

$$\omega_{n3} = \sqrt{\frac{\rho g A_w}{M + m_{33}^a}}, \quad \omega_{n5} = \sqrt{\frac{W \cdot \overline{GZ}_l}{I_{55} + J_{55}^a}} \tag{7}$$

Meanwhile, the heave wave damping coefficient is defined by $B_{33} = \rho g^2 \overline{A}^2 / \omega_w^3$ with $\overline{A}$ being the relative amplitude of radiation wave to the heave amplitude. And, the heave wave force and the wave-induced pitch moment are calculated by $Re\left(F_3 e^{i\omega_w t}\right) = W\gamma \cos\omega_w t$ and $Re\left(F_4 e^{i\omega_w t}\right) = W \cdot \overline{GZ}\gamma\Theta \cos\omega_w t$ respectively with γ being the effective wave slope coefficient and the peak wave slope: $\Theta=4\pi h_w/\lambda$ (Biran 2003, Lee 2003).

Substituting these relations into Eqs. (5) and (6) and dividing the resulting equations by $\left(M + m_{33}^a\right)$ and $\left(I_{55} + J_{55}^a\right)$ respectively lead to two decoupled second-order ODEs given by

$$\ddot{\eta}_3 + 2\zeta_3\dot{\eta}_3 + \omega_{n3}^2\eta_3 = \omega_{n3}^2\gamma \cos\omega_w t \tag{8}$$

$$\ddot{\eta}_5 + 2\zeta_5\dot{\eta}_5 + \omega_{n5}^2\eta_5 = \omega_{n5}^2\gamma \frac{4\pi h_w}{\lambda} \cos\omega_w t \tag{9}$$

to solve the rigid heave and pitch responses $\eta_3(t)$ and $\eta_5(t)$ of floating wind turbine. Here,

$\zeta_3 = (\rho g\overline{A}) / 2(M + m_{33}^a)$ and $\zeta_5 = (W \cdot \overline{GZ}_L) / 2(I_{55} + J_{55}^a)$ are the linear heave and pitch damping ratios, respectively. Eqs. (8) and (9) can be analytically solved when the natural heave and pitch frequencies ω_{n3} and ω_{n5} of floating wind turbine are known for a given 1-D harmonic wave and the linear damping ratios ζ_3 and ζ_5.

3.2 FE approximation of flexible structural dynamic response

The absolute dynamic displacement $\boldsymbol{z}(\boldsymbol{x};t)$ at a point $\boldsymbol{x}$ within the flexible spar-type floating wind turbine subject to the rigid body pitch and heave motions acting on the center of mass is expressed by

$$\boldsymbol{z}(\boldsymbol{x};t) = \eta_3 \boldsymbol{k} + \boldsymbol{r}(\boldsymbol{x}) \times \eta_5(t)\boldsymbol{j} + \boldsymbol{u}(\boldsymbol{x},t) \tag{10}$$

where $\boldsymbol{r}(\boldsymbol{x})$ denotes the position vector to the point $\boldsymbol{x}$ from the center of mass. Then, the relative damped dynamic displacement $\boldsymbol{u}(\boldsymbol{x};t)$ of the flexible floating wind turbine with respect to the rigid body motion at the center of mass is governed by

$$\nabla \cdot \sigma(\boldsymbol{u}) - c\boldsymbol{u} + \boldsymbol{f} = \rho \frac{\partial^2}{\partial t^2} \{\boldsymbol{z} - \boldsymbol{r}(\boldsymbol{x}) \times \eta_5(t)\boldsymbol{i}\} \tag{11}$$

with the Cauchy stress tensor $\sigma(\boldsymbol{u})$, the structural damping coefficient c, the body force $\boldsymbol{f}$, and the mass density ρ.

Introducing N iso-parametric basis functions $\{\phi_j(x)\}$ to the Galerkin approximation of Eq. (11) leads to

$$([\boldsymbol{M}] + [\boldsymbol{M}_{add}])\ddot{\overline{\boldsymbol{u}}} + [\boldsymbol{C}]\dot{\overline{\boldsymbol{u}}} + [\boldsymbol{K}]\overline{\boldsymbol{u}} = -([\boldsymbol{M}] + [\boldsymbol{M}_{add}])(\boldsymbol{r} \times \ddot{\eta}_4 \boldsymbol{i}) \tag{12}$$

Furthermore, in the space of eigen modes, the damped dynamic displacement can be expressed as a linear combination of natural modes $\Phi_j(\boldsymbol{x})$ and the modal participation coefficients $q_t(t)$

$$\overline{\boldsymbol{u}}(\boldsymbol{x};t) = \sum_{j=1}^{N} q_j(t) \cdot \Phi_j(\boldsymbol{x}) \tag{13}$$

By letting ($[\boldsymbol{M}]$+$[\boldsymbol{M}_{add}]$) be $[\tilde{M}]$, Eq. (12) can be rewritten as

$$\sum_{j=1}^{N} \left\{ [\tilde{\boldsymbol{M}}]\boldsymbol{\Phi_j}\ddot{q}_j + [\boldsymbol{C}]\boldsymbol{\Phi_j}\dot{q}_j + [\boldsymbol{K}]\boldsymbol{\Phi_j} q_j \right\} = \boldsymbol{P_{eff}} \tag{14}$$

with the effective dynamic force defined by

$$\boldsymbol{P}_{eff} = -[\tilde{\boldsymbol{M}}](\ddot{\eta}_3 \boldsymbol{k} + \boldsymbol{r}(\boldsymbol{x}) \times \ddot{\eta}_5 \boldsymbol{i}) \tag{15}$$

Multiplying Φ_k to Eq. (14) and using the M-orthonormality of the eigen modes, one can easily obtain the N decoupled second-order ODEs given by

$$\ddot{q}_k(t) + 2\varsigma_k \omega_k \dot{q}_k(t) + \omega_k^2 q_k(t) = Q_k \tag{16}$$

to compute the participation coefficients q_k. In which, ς_k and Q_k(=Φ_k $\boldsymbol{P}_{eff}$) denote the damping ratio and the normalized force at the k-th natural mode of the flexible floating wind turbine, respectively.

4. Numerical experiments

A scale model of spar-type floating offshore wind turbine shown in Fig. 1(b) is taken for the numerical and experimental study. The scaling methodology for the floating substructure and the wind turbine was referred to the report by NREL (Jonkman 2009). It is manufactured with *Al alloy 7079* having the density ρ of 2.7×10^{-3} g/mm^3, except for the rotor blades manufactured with *ABS*. The total mass M of the scale model is 9.5 kg and three mooring lines manufactured with Nylon have the length of 3.2 m, the pre-tension of 0.37 kgf and the equivalent stiffness EA of 0.85 kgf/m. Three mooring cables are connected to the substructure at 167 mm above the center of mass, and the wave drag force is not taken into account. Two decoupled ODEs in Eqs. (8) and (9) are solved by MATLab while the structural dynamic analyses are carried out using a commercial FEM code, midas NFX (Midas IT 2011). Meanwhile, the wave length, the wave frequency and the wave height are set by λ=16.0 m, ω_w=1.57 rad/sec and $h_w/2$=0.61 m, respectively.

4.1 Added masses and wave damping coefficient

Fig. 4(a) represents the variation of added mass to the wave frequency for six rigid body motions of the scale model which were evaluated by a hydrodynamics code. It has been reported that the total added mass and its distribution are affected by the geometry, dimension, natural frequency and mode of structure interfaced with liquid (Cho *et al*. 2001). It is observed that the total added mass is biggest in surge and sway motions but it becomes negligible in heave and yaw motions, such that it is 10.5 kg in surge and sway motions while 5 kg in pitch and roll motions, respectively. Fig. 4(b) shows the variation of the wave damping coefficients in each rigid body motion to the wave frequency that were obtained by the panel method in a hydro code, where the dependence of wave frequency is observed to be significant when compared with the added mass. Surge, sway, pitch and roll motions show almost a quadratic increase of wave damping coefficients to the wave frequency, while the wave damping coefficients in heave and yaw

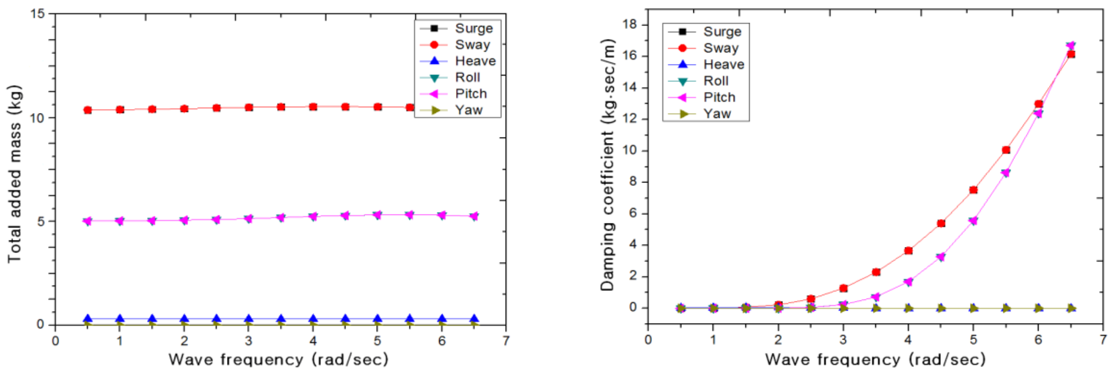

(a) (b)

Fig. 4 Frequency dependent added mass and damping coefficient of the spar floating substructure: (a) total added masses, (b) wave damping coefficients

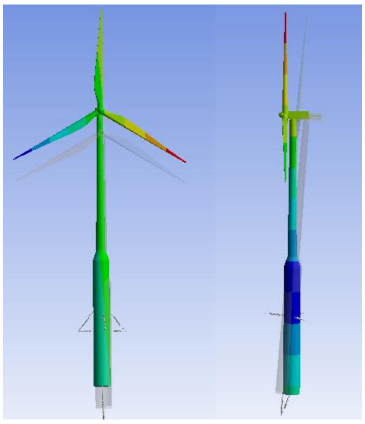

(a)

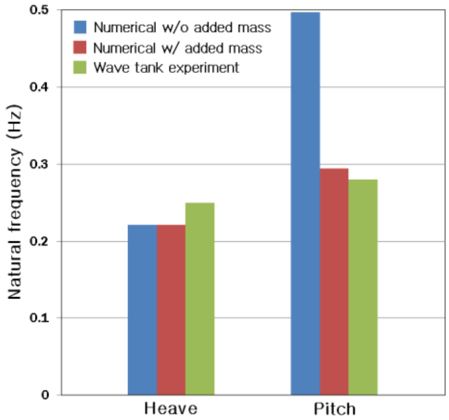

(b)

Fig. 5 Heave and pitch motions: (a) natural modes by finite element analysis, (b) comparison of natural frequencies

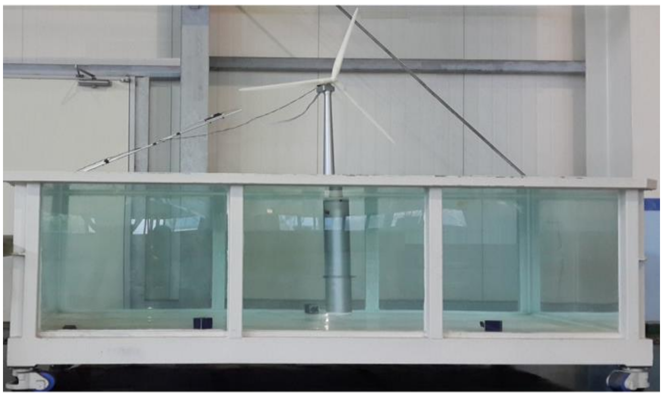

Fig. 6 A small-scale water tank for 1/100 scale floating offshore wind turbine.

motions are shown to be negligible as in case of the added mass. The wave damping coefficients at ω_w=1.57 rad/sec are taken and converted into the wave damping ratios by the critical wave damping ratios, in order to plug into Eqs. (8) and (9) for solving the time responses of rigid heave and pitch motions.

In order to verify the accuracy of added masses, the heave and pitch natural frequencies of the scale model between numerical and experiment are compared. The finite element modal analysis is carried out with and without considering the added mass, for which the added mass is applied to the outer surface of floating substructure as uniform distributed mass, as illustrated in Fig. 2. Meanwhile, the experiment of heave and pitch motions are performed within a specially designed small-scale water tank shown in Fig. 6. The heave and pitch natural models obtained by finite element analysis with the added mass are shown in Fig. 5(a), and the comparison of their natural frequencies with experiment is represented in Fig. 5(b). When compared with the experiment, the numerical simulation leads to lower natural frequency in heave motion and vice versa for pitch motion such that the maximum relative error with respect to the experimental data is 10.5%. Meanwhile, from the comparison of the numerical results with and without added mass, it is

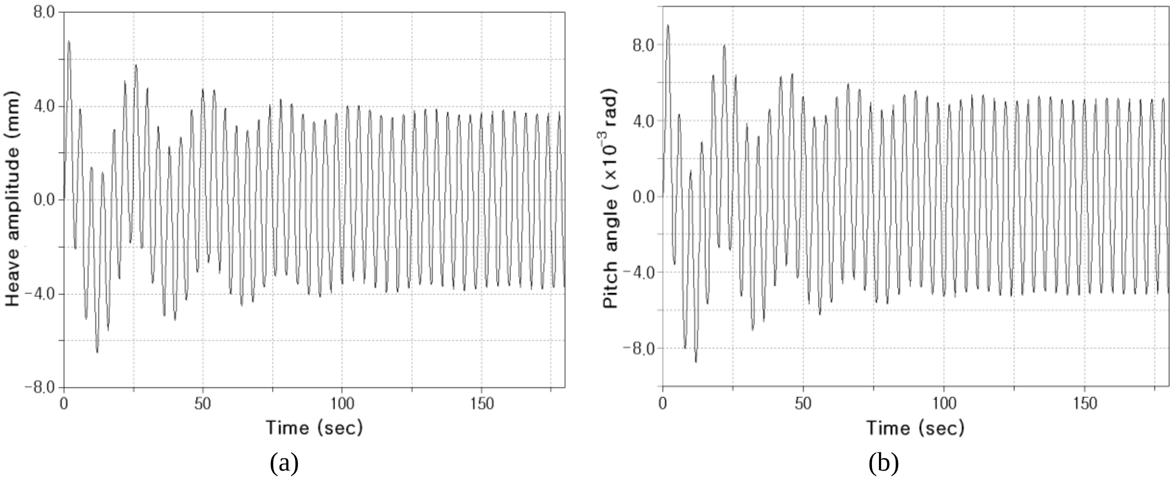

Fig. 7 Time histories of the wave-induced rigid body motion of spar-type floating wind turbine: (a) heave motion, (b) pitch motion

confirmed that heave motion does not show a noticeable difference but pitch motion produces the significantly lower natural frequency by relatively 40.9% when the added mass is considered.

4.2 Structural dynamic responses

Two decoupled ODEs in Eqs. (8) and (9) are solved using MATLab with the natural frequencies and wave damping ratios of the scale model in heave and pitch motions. The added masses for calculating the natural frequencies and the wave damping coefficients in heave and pitch motions are taken at the wave frequency ω_w=1.57 rad/sec from the plots shown in Fig. 4. The analytically solved time responses of rigid heave and pitch motions are represented in Figs. 7(a) and 7(b), respectively. It is observed that the rigid heave and pitch motions show the apparent transient response up to around $90\,sec$ owing to the pre-tensioned flexible three mooring cables. After that, both motions exhibit almost the steady-sate harmonic response with the extremely small decay in the amplitudes owing to the small wave damping given in Fig. 4(b). It was found from the detailed numerical results that the peak amplitudes are 6.77 mm in heave motion and 8.70×10^{-3} rad in pitch motion.

Next, the structural dynamic analyses of the spar-type floating wind turbine were carried out using a flexible finite element structural model shown in Fig. 2, for which the time responses shown in Fig. 7 of the rigid heave and pitch motions are applied to the center of mass of wind turbine. And, the buoyancy force acting on the bottom of substructure and the mooring force are modeled as linear springs with the spring constants which were determined according to the explanation given in Section 2.2. Meanwhile, one may use the unit load approach if the nonlinearity in the structural response can be neglected. The spar floating wind turbine is discretized with 20-node hexa, 10-node tetra and 2-node beam elements, and the total element and node numbers reach 52, 909 and 112,831, respectively. Referring to Fig. 3, the dynamic displacement is extracted from two points A and B of wind blades and the dynamic effective stress is taken from point *C*, where points *A* and *B* indicate the tips of two wind blades while point *C* denotes the fairlead position. Note that point *A* is aligned to the *z*-axis and point *C* directs to the

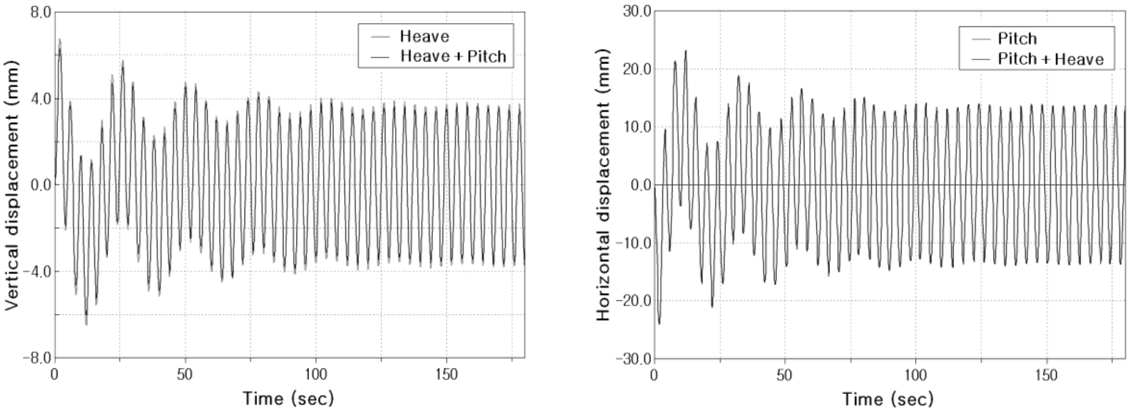

(a) (b)

Fig. 8 Time responses of the dynamic displacement at point A: (a) vertical displacement, (b) horizontal displacement

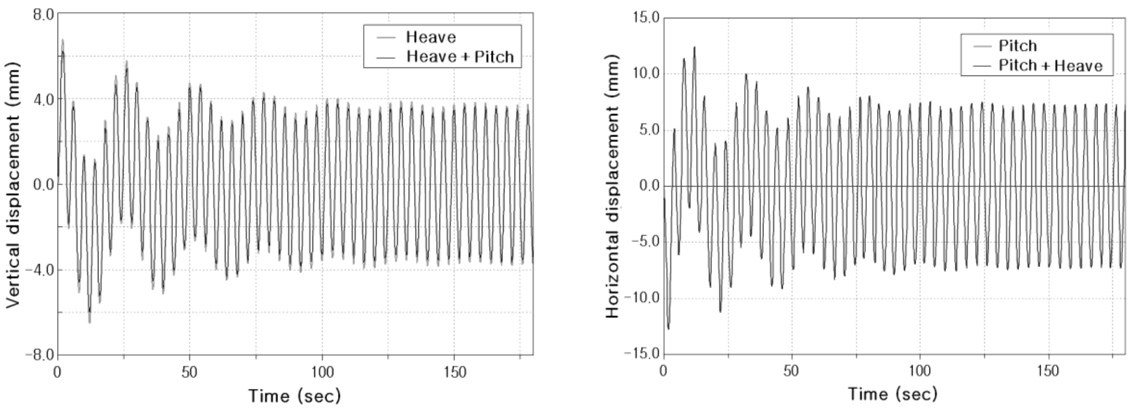

(a) (b)

Fig. 9 Time responses of the dynamic displacement at point B: (a) vertical displacement, (b) horizontal displacement

x-axis. The heave and pitch motions of the rigid floating substructure are specified to the flexural structural model *separately and simultaneously* to examine the coupling effect on the flexural structural responses between heave and pitch motions.

Fig. 8(a) represents the time histories of vertical displacement of wind blade at point A, where one is obtained by applying only the heave excitation while the other is due to the coupled heave and pitch excitation. First of all, it can be observed that both cases lead to almost the same time response as the rigid heave motion shown in Fig. 7(a). The peak responses are occurred at 1.87 sec in both cases, but the peak displacements are slightly different such that 6.77 mm for the pure heave excitation while 6.29 mm for the coupled heave and pitch excitation. Thus, it is found that the pitch motion gives rise to the coupling effect on the vertical displacement at point *A* such that the peak displacement is reduced by 7.1%. Fig. 8(b) shows the time histories of horizontal displacement at point *B*, where the difference between two excitation cases is observed to be too small to distinguish. Thus, it is found that the heave motion does not produce the remarkable

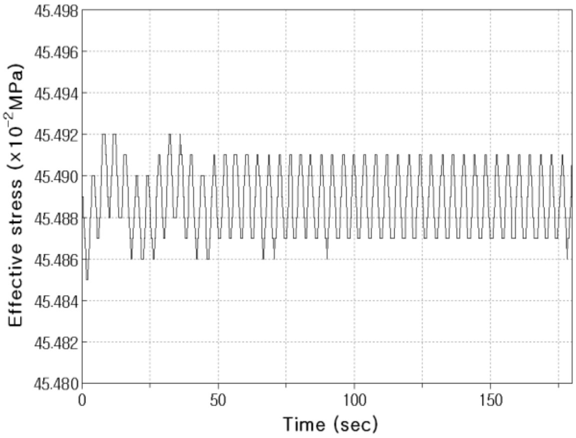

(a)

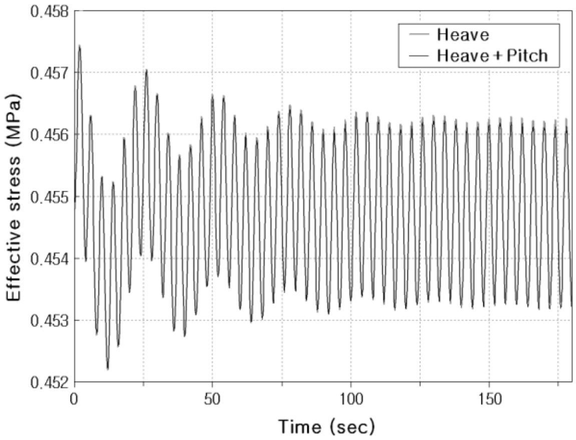

(b)

Fig. 10 Time responses of the effective stress at point C: (a) by pitch motion, (b) by heave and coupled heave and pitch motions

coupling effect on the horizontal displacement at point *A*, and both cases produce the peak displacement of 21.36 mm at 7.99 sec. The time histories of vertical and horizontal displacements at point *B* are represented in Fig. 9. The vertical displacement shows almost the same time response as point *A*, so that the peak response time, the peak displacement and the coupling effect by the pitch motion are almost the same. Meanwhile, the horizontal displacement shows the time response having the amplitude smaller than point *A*, because point *B* is positioned lower than point *A*.

Fig. 10(a) represents the time history of effective stress at point *C* due to the pitch excitation, where the mean stress of 49.849×10^{-3} MPa is caused by the tension of three mooring lines. This mean stress value can be also observed from Fig. 10(b) for the cases when the pure heave excitation and the coupled heave and pitch excitation are applied. It is found that the pitch excitation produces the stress variation ranging from 0.009×10^{-3} MPa to 0.0076×10^{-3} MPa which is significantly smaller than the mean stress. Differing from the pitch excitation, the heave excitation produces the remarkable stress variation ranging from 0.003 MPa to 0.0052 MPa, implying that the variation of effective stress at point *C* is dominated by the heave excitation. It is because the effective stress at point *C* is caused by the mooring line tension which is in turn influenced by the extension amount of mooring cables. It can be observed from Fig. 10(b) that the coupling between heave and pitch motion reduces the stress variation but its influence is negligible because the stress variation itself caused the pitch excitation is extremely small. Meanwhile, it was observed that the time histories of effective stress at other two fairlead positions having the 120° spacing are almost the same as point *C*, except that the stress variation by the pitch excitation becomes smaller.

5. Conclusions

A semi-analytical numerical approach has been introduced in this paper to effectively analyze the structural dynamic response of 1/100 scale model of spar floating substructure subject to wave-induced excitation. The decoupled second-order ordinary differential equations governing the rigid heave and pitch motions were derived from the generalized equations of rigid ship motion. The rigid heave and pitch motions of spar floating substructure at sea state 3 which were analytically solved were applied to the center of mass of floating structure as external dynamic loads, and then the structural dynamic responses of the flexible floating substructure were analyzed by the finite element method. The hydrodynamic interaction between wave and structure was taken into consideration by means of the added mass and the wave damping, and its modeling accuracy was verified from the comparison of natural frequencies of the 1/100 scale model of floating wind turbine.

It has been observed that the rigid heave and pitch motions at sea state 3 show the apparent transient response up to around 90 sec owing to the pre-tensioned flexible three mooring cables. After that, both motions exhibit almost the steady-sate harmonic response with the small decay in the amplitudes. Meanwhile, it has been observed, from the time responses of displacement at two blade tips, that the pitch motion gives rise to the coupling effect on the vertical tip displacement such that the peak vertical displacement is reduced by 7.1%. But, the heave motion does not produce the coupling effect on the horizontal tip displacement. Restricted to point A of wind blade, the peak vertical displacement was 6.77 mm at 1.87 sec while the peak horizontal displacement was 21.36 mm at 7.99 sec. From the time history of effective stress at the fairlead position aligned to the wave direction, it has been found that the mean stress caused by the mooring line tension is 49.489×10^{-3} MPa. And, the stress variation with time is dominated by the heave motion such that the stress variation by heave motion is over one thousand times as large as one by pitch motion. It is consistent well with the fact that the effective stress at the fairlead position is caused by the mooring line tension which is in turn influenced by the mooring cable extension. Furthermore, it has been observed that the coupling between heave and pitch motion reduces the stress variation even though the stress reduction is insignificant.

The current study has been limited to the heave and pitch motions, but the surge and pitch motions and their coupling effect are also important for the structural dynamic response analysis of spar floating substructure. It represents a topic that deserves future work.

Acknowledgements

This work was supported by the Human Resources Development of the Korea Institute of Energy Technology Evaluation and Planning (KETEP) grant funded by the Korea Ministry of Knowledge Economy (No. 20113020020010).

References

Biran, A.B. (2003), *Ship Hydrostatics and Stability*, Butterworth-Heinemann, Singapore.

Cho, J.R., Han, K.C., Hwang, S.W., Cho, C.S. and Lim, O.K. (2012), "Mobile harbor: structural dynamic response of RORI crane to wave-induced rolling excitation", *Struct. Eng. Mech.*, **43**(5), 679-690.

Cho, J.R., Song, J.M. and Lee, J.K. (2001), "Finite element techniques for the free-vibration and seismic analysis of liquid-storage tanks", *Finite Elem. Anal. Des.*, **37**, 467-483.

Colwell, S. and Basu, B. (2009), "Tuned liquid column dampers in offshore wind turbines for structural control", *Eng. Struct.*, **31**, 358-368.

Faltinsen, O.M. (1990), *Sea Load on Ships and Offshore Structures*, University of Cambridge.

Goopee, A..J., Koo, B..J., Lambrakos, K.F. and Kimball, R.W. (2012), "Model tests for three floating wind turbine concepts", *Proceedings of Offshore Technology Conference*, Houston, USA.

Hansen, A.D. and Hansen, L.H. (2007), "Wind turbine concept market penetration over 10 years (1995-2004)", *Wind Energy*, **10**, 81-97.

Jensen, J., Olsen, A. and Mansour, A. (2011), "Extreme wave and wind response predictions", *Ocean Eng.*, **38**, 2244-2253.

Jeon, S.H., Cho, Y.U., Seo, M.W., Cho, J.R. and Jeong, W.B. (2013), "Dynamic response of floating substructure of spar-type wind turbine with catenary mooring cables", *Ocean Eng.*, **72**, 356-364.

Jonkman, J. (2009), "Definition of the floating system for phase IV of OC3", Technical Report NREL/TP-500-47535.

Jonkman, J. (2009), "Dynamics of offshore floating wind turbines-model development and verification", *Wind Energy*, **12**, 459-492.

Jonkman, J. and Musial, W. (2010), "Offshore code comparison collaboration (OC3) for IEA task 23 offshore wind technology and development", Technical Report NREL/TP-5000-48191, Colorado.

Karimirad, M., Meissonnier, Q., Gao, Z. and Moan, T. (2011), "Hydroelastic code-to-code comparison for a tension leg spar-type floating wind turbine", *Marine Struct.*, **24**, 412-435.

Koo, B.J., Kim, M.H. and Randall, R.E. (2004), "Mathieu instability of a spar platform with mooring and risers", *Ocean Eng.*, **31**, 2175-2208.

Lee, S.G. (2003), *Ship Motion and Maneuverability*, Pusan National University Press, Busan. (in Korean)

Lee, S.H. (2008), "Dynamic response analysis of spar buoy floating wind turbine systems", Ph.D. Thesis, MIT.

Lee, H.H., Wong, S.H. and Lee, R.S. (2006), "Response mitigation on the offshore floating platform system with tuned liquid column damper", *Ocean Eng.*, **33**, 1118-1142.

Li, Y. and Kareem, A. (1990), "Stochastic response of tension leg platforms to wind and wave fields", *J. Wind Eng. Indus. Aerodyn.*, **36**(2), 915-926.

Midas IT. (2011), *User's Manual of Midas NFX*, Gyeonggi, Korea.

Pierson, W.J. and Moskowicz, L. (1964), "A proposed spectral form for fully developed wind seas based on the similarity theory of S.A. Kitaigorodskii", *J. Geophys. Res.*, **69**(24), 5181-5203.

Tong, K.C. (1998), "Technical and economic aspects of a floating offshore wind farm", *J. Wind Eng. Indus. Aerodyn.*, **74-76**, 399-410.

Tracy, C. (2007), "Parametric design of floating wind turbines", Maters Thesis, MIT.

Utsunomiya, T., Matsukuma, H. and Minoura, S. (2010), "On sea experiment of a hybrid SPAR for floating offshore wind turbine using 1/10 scale model", *Proceedings of ASME 2010 29th International Conference on Ocean*, Offshore and Artic Engineering, Shanghai, China.

Wang, L. and Sweetman, B. (2012), "Simulation of large-amplitude motion of floating wind turbines using conservation of momentum", *Ocean Eng.*, **42**, 155-164.

CC